

TABLE II. Computed values of  $f_0(\text{Eu})$  derived from different diffraction peaks.

$hkl$	Scattering angle	Structure factor <sup>a</sup>	Multiplicity	$P_{hkl}$ <sup>b</sup>	$F_{hkl}^2$ ( $10^{-12} \text{ cm}^2$ )	$f_0(\text{Eu})$ ( $10^{-12} \text{ cm}$ )
222	25.6°	$0.43 f_0 - 30.31 f_{\text{Eu}}$	8	$593 \pm 20$	$274 \pm 30$	$0.80 \pm 0.05$
332	35.0°	$14.90 f_0 + 2.95 f_{\text{Eu}}$	24	$366 \pm 25$	$101 \pm 20$	$0.72 \pm 0.08$
440	42.3°	$31.60 f_0 + 27.67 f_{\text{Eu}}$	12	$1320 \pm 100^c$	$1020 \pm 200$	$0.74 \pm 0.08$

<sup>a</sup> Structure factor calculated for  $x=0.370$ ,  $y=0.155$ ,  $z=0.405$ , and  $u=-0.030$ . The Debye-Waller temperature factor has been omitted in this tabulation.

<sup>b</sup>  $P_{hkl}$  is proportional to the area under the diffraction peaks.

<sup>c</sup> This value of  $P_{440}$  has been corrected for the contribution of the adjacent (521) peak.

served at the Bragg angle corresponding to the (400) plane; since the structure factor is  $F_{400} \cong 30f_{\text{Eu}} - 45f_0$ , it can be concluded that Eu scatters with the same phase as oxygen or positive phase. Additional confirmation of the phase is established by the large peak at 42.3° which is primarily due to the (440) plane; the

structure factor,  $F_{440} = 27.7f_{\text{Eu}} + 31.6f_0$ , again indicates that Eu and O scatter with the same phase.

#### ACKNOWLEDGMENT

The authors wish to thank Charles Critchfield for helpful discussions.

### Single-Quantum Annihilation of Positrons\*

L. SODICKSON,<sup>†</sup> W. BOWMAN,<sup>†</sup> AND J. STEPHENSON<sup>†</sup>

*Physics Department and Laboratory of Nuclear Science, Massachusetts Institute of Technology, Cambridge, Massachusetts*

AND

R. WEINSTEIN

*Northeastern University, Boston, Massachusetts*

(Received May 18, 1960)

An experiment has been performed to investigate single-quantum annihilation of positrons in the field of high- $Z$  nuclei. This mode of annihilation has been observed and the absolute magnitude, energy dependence, and  $Z$  dependence of the cross section measured. Backgrounds which might contaminate the derived signals have been semiempirically investigated and found to be an order of magnitude or more below the rate identified as single-quantum annihilation. The data on absolute magnitude of the counting rate and its dependence on positron energy agree with the calculations of Jaeger and Hulme. The  $Z$  dependence agrees with a cross section proportional to  $Z^5$ .

#### I. INTRODUCTION

ANNIHILATION of an electron-positron pair can take place via the emission of one, two, three, or more quanta. In solids, the most probable mode is two-quantum annihilation of a positron electron pair almost at rest.<sup>1,2</sup> This accounts for all but a few percent (e.g., 3%) of positrons from typical radioactive sources, when the positrons are stopped in metals. In this case, two-

quantum annihilation in flight<sup>1,3,4</sup> accounts for most of the remaining positrons.

Three-quantum annihilation occurs from the  $^3S_1$  state of the  $e^+e^-$  system. This is a consequence of conservation of angular momentum, and the transverse nature of the electromagnetic field. Three quantum annihilation is profuse in those gases (e.g., argon) not capable of causing transitions to the more rapidly annihilating  $^1S_0$  state. Indeed, under certain conditions of external field<sup>5</sup> annihilation via three quantum emission occurs nearly 75% of the time.

There are no other profuse annihilation modes. Annihilation via the emission of more than three quanta

\* Supported in part by funds provided by the USAEC, The Air Force Office of Scientific Research, and the Office of Naval Research.

<sup>†</sup> Submitted in partial fulfillment of the requirements for the degree of Bachelor of Science at Massachusetts Institute of Technology, Cambridge, Massachusetts.

<sup>1</sup> W. Heitler, *Quantum Theory of Radiation* (Oxford University Press, New York, 1954), 3rd ed., pp. 268-272.

<sup>2</sup> S. DeBenedetti, C. Cowan, W. Konneker, and H. Primakoff, *Phys. Rev.* **77**, 205 (1950).

<sup>3</sup> J. Gerhart, B. Carlson, and R. Sherr, *Phys. Rev.* **94**, 917 (1954).

<sup>4</sup> H. Kendall and M. Deutsch, *Phys. Rev.* **101**, 20 (1956).

<sup>5</sup> M. Deutsch, *Progress in Nuclear Physics* (Butterworths Scientific Publications, Ltd., London, 1953), Vol. 3.

is always possible, but is inhibited with respect to one-, two-, or three-quantum emission by one or more powers of the fine-structure constant, since under any experimental conditions, one of the latter modes of annihilation is always possible.

One-quantum annihilation is forbidden, for real processes, for a free  $e^+e^-$  pair, due to the impossibility of balancing both momentum and energy simultaneously. Under these circumstances, single-quantum annihilation (hereafter denoted SQA) can still contribute to virtual processes in which momentum, but not energy, is balanced. Indeed, this virtual process accounts for a large fraction of the fine-structure splitting in positronium.<sup>6-8</sup>

In the presence of a third body, e.g., a nucleus, SQA is allowed since the third body can recoil and allow simultaneous momentum and energy conservation. Indeed, SQA is expected<sup>9-11</sup> to account for up to 0.2% of positron annihilations in high- $Z$  targets for typical radioactive sources.

The matrix element, in the Born approximation, is proportional to  $Z^{\frac{1}{2}}$  and gives rise to a cross section of magnitude approximately  $\alpha^4 Z^5 r_0^2$ , where  $\alpha$  is the fine-structure constant and  $r_0$  the classical electron radius. In this strong  $Z$  dependence, the normalization of the electron wave function gives rise to  $Z^3$  dependence in the matrix element. This follows since the volume around the nucleus in which the electron is confined, essentially a sphere of the Bohr radius, varies as  $Z^{-3}$ . As a result electrons in other than the  $K$  shell have negligible cross sections for SQA, and SQA is usually accompanied by  $K$  x-ray emission.

Several attempts have been made to observe SQA.<sup>3,12-14</sup> Meric<sup>12</sup> and Whalen<sup>14</sup> may have had a measure of success. Meric, in an early experiment on one- and two-quantum annihilation in flight, demonstrated by means of an absorption technique the existence, in annihilation radiation, of a high-energy gamma-ray component which was more prevalent in Pb than in Al. Whalen, in an experiment qualitatively like the one here described, measured a lead-aluminum difference for a hard and soft gamma in coincidence. Experiments are hampered by the rarity of the event and the necessarily large background rates. In Whalen's experiment, for example, signal rates of 0.1 count per minute were sought in a background three times as

large. The observed signal, attributed to SQA, gave a cross section approximately twice the theoretical value.<sup>10</sup> Due to the low counting rates it was impossible to collect data on any high- $Z$  target but Pb, and consequently no check of  $Z$  dependence was made.

The experiment described herein was undertaken as and exploratory measurement<sup>15</sup> to clearly identify SQA and measure the dependence of the cross section on target  $Z$  and on positron kinetic energy,  $E^+$ . The experiment was carried to the point where a major redesign became necessary in order to remove factors limiting the accuracy of the measurements (see Sec. V).

## II. THE EXPERIMENT

The experiment, conceptually, can be performed in two ways. A "thin-target experiment" may be done in which only those annihilations are observed which occur for a differential range of positron energies. The event may be identified by the high-energy gamma ray, the emission of a  $K$  x ray, and, if the positron energy is sufficient, by the arrival of a positron. The angular distribution<sup>16</sup> of the resulting gamma may be measured in addition to the dependence of the cross section on positron kinetic energy ( $E^+$ ) and on target  $Z$ .

The background situation in the present experiment did not permit a thin-target measurement to be made. The requirement of a thin target implies low rates for source strengths permitted by background requirements; hence a thick-target experiment was performed. In a thick-target experiment the incident positrons are slowed down and, if not annihilated in flight, stopped in the target. Their direction of motion becomes isotropic soon after entering the target. In losing, typically, 5% of energy, positron directions become isotropic.<sup>17</sup> Hence, one cannot check the angular distribution of the gamma rays from SQA in a thick-target experiment. Annihilation is observed for all positron energies below the energy of the incident positron. Triggering on an incoming positron is impractical, and only the resulting energies of the gamma ray and the x ray are used to identify SQA. This type of experiment is reported on here. Biases were set to observe SQA for almost the entire range of energies through which the positrons pass in coming to rest.

One-quantum annihilation of a positron gives rise to a single hard quantum of energy

$$E_{1\gamma} = 2m_0c^2 + E^+ - I_k, \quad (1)$$

where  $m_0$  is the electron rest mass,  $E^+$  is the kinetic energy of the positron, and  $I_k$  is the  $K$ -shell ionization energy of the target atoms. (The very small recoil energy of the nucleus is neglected here.) For example, for a lead target, and positrons incident with kinetic

<sup>6</sup> R. Karplus and A. Klein, *Phys. Rev.* **87**, 848 (1952).

<sup>7</sup> R. Weinstein, M. Deutsch, and S. C. Brown, *Phys. Rev.* **94**, 758(A) (1954); *Phys. Rev.* **98**, 233A (1955).

<sup>8</sup> V. Hughes, S. Marder, and C. S. Wu, *Phys. Rev.* **106**, 934 (1957).

<sup>9</sup> W. Heitler, see reference 1, pp. 272-274.

<sup>10</sup> J. Jaeger and H. Hulme, *Proc. Cambridge Phil. Soc.* **32**, 158 (1936).

<sup>11</sup> E. Fermi and G. Uhlenbeck, *Phys. Rev.* **44**, 510 (1933).

<sup>12</sup> S. Meric, *Rev. fac. sci. univ. Istanbul* **15**, Part I, 136 (1950); Part II, 179 (1950).

<sup>13</sup> D. Farmer and J. Streib, *Phys. Rev.* **96**, 855 (1954).

<sup>14</sup> J. Whalen, Ph.D. thesis, Washington University, St. Louis, Missouri, 1955 (unpublished).

<sup>15</sup> R. Weinstein, *Bull. Am. Phys. Soc.* **4**, 325 (1959).

<sup>16</sup> Y. Nishina, S. Tomonaga, and H. Tamaki, *Sci. Papers Inst. Phys. Chem. Research, Tokyo* **24**, No. 18 (1934).

<sup>17</sup> H. A. Bethe, *Proc. Roy. Soc. (London)* **A150**, 129, 1935 and F. Rohrlich and B. Carlson, *Phys. Rev.* **93**, 38 (1954).

energy  $E_0^+ = 400$  keV,

$$0.932 \text{ MeV} \leq E_{1\gamma} \leq 1.332 \text{ MeV}.$$

The lower limit corresponds to SQA at rest. Biases were actually set to accept gamma-ray energies from 1.05 MeV to 1.40 MeV. The lower bias was set due to background considerations, as explained in Sec. VII.

For comparison, the most energetic gamma from 2-quantum annihilation in flight is

$$E_{2\gamma, \text{max}} = 1.09 \text{ MeV}.$$

It should be noted that as the energy of the positron is increased, the SQA quantum and the highest energy quantum from two-quantum annihilation in flight approach an asymptotic value of energy difference of just 0.25 MeV. (This asymptotic value is very nearly achieved at  $E^+ = 250$  keV.) Thus as  $E^+$  increases the (2-quantum)–(1-quantum) energy difference becomes a monotonically decreasing *fraction* of the SQA energy. This makes rejection of two-quantum annihilation in flight an increasingly difficult task as  $E^+$  increases. This argues for doing an exploratory measurement at low  $E^+$ . In the experiment described here there is strong evidence that two-quantum annihilation in flight is practically completely rejected. (See Sec. VII.)

The SQA rates are very low compared to two-quantum annihilation at rest and in flight. It is desirable to select a portion of the beta-ray spectrum in which the background singles events from two-quantum annihilation contribute least to a spurious SQA rate. The lower portion of the beta spectrum is poor because the cross section for SQA falls sharply at low beta energies (see Fig. 4), and hence these betas contribute to the background but not to the signal. We desire to eliminate the low-energy source betas in order to maximize signal to noise. The upper portion of a beta spectrum is poor because in this energy region the hard gammas from SQA and two-quantum annihilation in flight have a small fractional energy difference. We desire to choose, for this experiment, a beta energy such that, even in a thick-target experiment, the highest energy quanta from two-quantum annihilation in flight may be separated from the lowest energy quanta observed from SQA. Such criteria require the ability to cut out the high-energy portion of the beta spectrum. One also desires to remove the target for SQA from the positron source in order to avoid background contributions by hard nuclear gammas. (See Sec. VII on backgrounds.) For these reasons, it is necessary to use a beta-ray spectrometer.

Schematically, the experiment is as follows: (See Fig. 1.) A beam of positrons with a small fractional spread in energy is allowed to strike a thick target. The positrons are stopped in the target. Before stopping, they can undergo fast two-quantum or one-quantum annihilation. Those positrons which stop, annihilate almost entirely by two-quantum annihilation.

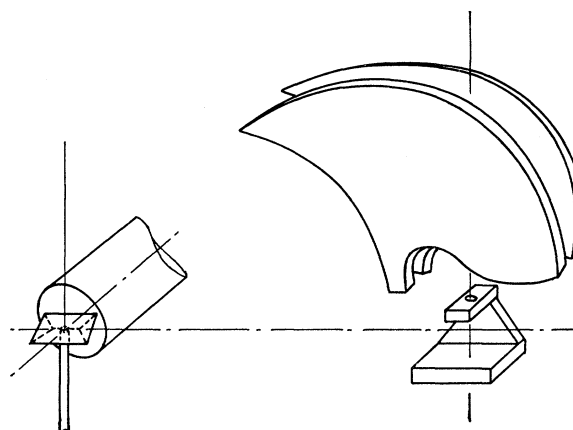


FIG. 1. Schematic diagram of vacuum chamber, double focusing magnet (upper right), source holder (directly below magnet), and target on externally controlled axis (lower left). The cylindrical thin detector window for the gamma counter can be seen behind the target. During normal operation lead shielding is placed in the region of the direct line from source to detectors. All high- $Z$  shielding is clad in tin or aluminum.

SQA with a  $K$ -shell electron is identified by simultaneous observation of the annihilation gamma ray and the  $K$  x ray. A characteristic  $K$  x ray is emitted after most ( $>96\%$ ) of the  $K$  ionizations.<sup>18</sup>

### III. EQUIPMENT

In order to provide a momentum-analyzed beta flux, an orange peel spectrometer was constructed<sup>19</sup> with poor resolution (3%) and high collection efficiency (3.5%). Targets 2 in.  $\times$  1.4 in. were used. The positrons striking these targets defined the incident positron energy to about  $\pm 6\%$ . Approximately 1 Mc of  $\text{Na}^{22}$  was used as a source of positrons. At  $E_0^+ = 400$  keV, for example,  $6.6 \times 10^4$  positrons/sec were incident upon the targets. The spectrometer focusing was studied at considerable length and will be reported on elsewhere. The spectrometer source, targets, and source shielding (lead and heavy metal) were inclosed in a vacuum chamber (see Fig. 1). The targets were mounted on spokes of a wheel, the axis of which was mounted on a Wilson seal. Four targets were mounted at any one time, and hence four different target  $Z$ 's could be intercompared without opening the vacuum system. Targets of Ta, W, Pt, Au, Pb, Th, and Al were used. The thorium target was a jigsaw combination of many small areas of thorium. This target required special analysis because (a) it intercepted only certain portions of the  $\beta$  flux compared to the other targets and (b) the natural radioactivity creates a special spurious SQA signal which had to be separately measured.

The actual targets were thin foils mounted on alumi-

<sup>18</sup> I. Bergström, *Beta- and Gamma-Ray Spectroscopy*, edited by K. Siegbahn (Interscience Publishers, Inc., New York, 1955), p. 630.

<sup>19</sup> W. Bowman, S. B. thesis, Massachusetts Institute of Technology, Cambridge, Massachusetts, Physics Department, 1957 (unpublished).

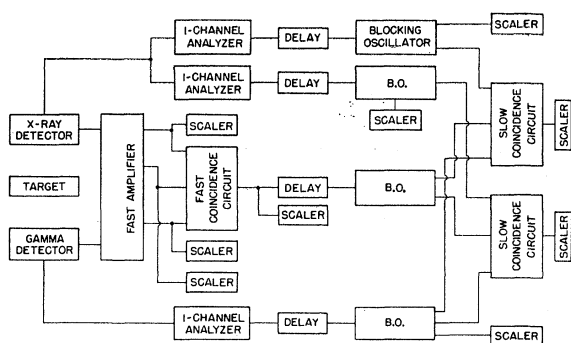


FIG. 2. Block diagram of electronics.

num holders. The foil thickness in each case was slightly greater than the extrapolated range of the betas.

The gamma-ray and x-ray detectors were potted NaI(Tl) crystals. The gamma detector was a cylinder 2 in. in diameter and 2 in. long axially mounted on an RCA6810 photomultiplier. The x-ray detector was 2 in. in diameter and 2 mm thick, and was mounted on an RCA7265 photomultiplier. The thin detector had about 90% efficiency for lead  $K$  x rays and about 5% efficiency for the detection of a 0.51-Mev quantum in which the pulse resulting from a Compton interaction with the detector fell within our x-ray pulse height window.

A block diagram of the electronics is shown in Fig. 2. A fast diode coincidence circuit ( $10^{-7}$  sec) was used in parallel with a slow coincidence circuit ( $3 \times 10^{-6}$  sec). The fast coincidence circuit was limited to  $10^{-7}$  sec because of our desire to do some crude pulse-height analysis even on the fast part of the circuit. The slow coincidence circuit required a threefold coincidence between the output of the fast circuit and the outputs of the pulse height analyzers. For the fast coincidence, the anode pulses from the detectors are fed to EFP60 discriminator circuits and then to a  $10^{-7}$  sec diode coincidence circuit. In addition, pulses are taken from the 14th dynode of each phototube and are fed through cathode followers to single-channel analyzers. The outputs of the analyzers and the fast coincidence circuit are put into a slow ( $3 \mu\text{sec}$ ) coincidence circuit.

The window of the gamma detector was run so as to include nearly all possible energies of the gamma rays resulting from SQA of a positron of energy less than  $E_0^+$ . Although the lowest observable SQA gamma from (e.g.) Pb, is 0.932 Mev, the lower bias level was actually run at 1.050 Mev because of background considerations (see Sec. VII). This has very little effect on the integral SQA counting rate, and the effect was included in comparisons with the theory (Sec. VI). For the purpose of simultaneously monitoring background, the x-ray output is fed into two single-channel analyzers. Each is utilized in a logic circuit such as described above. The window of the first x-ray differential discriminator was run centered on the x-ray peak of the target element. The second x-ray channel was normally run above the

$K$  x-ray peak of the target. The two x-ray channels were compared and, when set with equal biases, gave the same SQA rate to better than 0.5%.

All observable singles and coincidence rates were monitored with scalars.

#### IV. CALIBRATION

##### Spectrometer

The spectrometer was momentum calibrated with a  $\text{Bi}^{207}$  electron source. The spectrum of  $\text{Na}^{22}$  was then observed by measuring the target connected rate of 0.51-Mev annihilation quanta. The spectrum observed in this way was in reasonable agreement with other measurements in the literature<sup>20,21</sup> within the experimental errors of the present measurements. The  $\text{Na}^{22}$  spectrum was in good agreement with the more accurate  $\text{Bi}^{207}$  calibration. For example, the  $\text{Bi}^{207}$  calibration indicated that 400-keV positrons should correspond to 97 gauss on our field monitor, while the  $\text{Na}^{22}$  spectrum indicated that 400-keV positrons corresponded to a monitor reading of  $97 \pm 7$  gauss.

The agreement of the  $\text{Na}^{22}$  spectrum measured as described above with those in the literature is an experimental indication that the observed 0.51-Mev rate may be used as a measure of the positron flux vs positron energy for a given target. This is equivalent to assuming that, for a given target, the back-scattered fraction is not a function of the incident positron energy. This assumption has been found to be approximately valid by others.<sup>22</sup>

The flux of positrons in this experiment is taken to be the target-in minus the target-out rate of the 0.51-Mev photopeak, divided by the efficiency of the detector for 0.51-Mev quanta, and divided by the backscatter coefficient.<sup>22</sup> The positron flux was *not* directly measured. It was felt that the uncertainties in the calculations (see Sec. VI) did not merit this additional measurement.

A target of length 2 in. and width 1.4 in. was used to collect the positrons. A study of the focal properties of the magnet at the target position was made using a  $\text{Bi}^{207}$  electron source and this information was used to compute the momentum spectrum of positrons striking the target. The major characteristic of this spectrum was a full energy width at half maximum of 6%.

In the final computation of cross section, the efficiencies of the detectors enter. Since this is a function of the location of the event on the rather large target, the target was divided into 35 smaller areas, and theoretical source distribution weights were assigned to each position on the basis of the experimental studies of the magnets focal properties. A crude check on these calcu-

<sup>20</sup> W. Good, D. Peaslee, and M. Deutsch, *Phys. Rev.* **69**, 313 (1946).

<sup>21</sup> P. Macklin *et al.*, *Phys. Rev.* **78**, 318(A) (1950).

<sup>22</sup> H. Seliger, National Bureau of Standards Circular No. 527 (U. S. Government Printing Office, Washington, D. C. 1954), p. 86.

lations was made by exposing a photographic plate to the incident beta flux from Na<sup>22</sup>. The resulting picture shows an exposure density in agreement with the computed weights, well within the accuracy of this measurement.

The spatial distributions computed as described above were used in the computation and measurement of the average efficiency times solid angle ( $\langle\epsilon\Omega/4\pi\rangle$ ) for the x and gamma ray detectors. e.g.,

$$\langle\epsilon\Omega/4\pi\rangle_\gamma = \sum_n W_n [\epsilon_n \Omega_n / 4\pi]_\gamma,$$

where  $W_n$  are the computed (normalized) positron source weights for the 35 subunits of the targets and  $\epsilon_n \Omega_n$  are the computed or measured efficiency times solid angle of the gamma-ray detector for the  $n$ th target subarea. A separate computation of this type was carried out for the tungsten target because it was composed of a jigsaw puzzle of tungsten with some gaps. These gaps changed the source weights attributed to various points on the target.

### Detectors

The x-ray detector efficiency was determined semi-empirically by using a calibrated source of 88-keV  $\gamma$  rays from Cd<sup>109</sup>. The efficiency was measured, and a weighted average efficiency was taken over the 35 target positions as described in the previous section. It should be noted that the efficiency measurements were made *in situ*, and include the effect of thin aluminum vacuum chamber walls. This effect, denoted  $\delta$  ( $Z$ ), is dependent on the energy of the x rays used to calibrate the detector. The weighted average of the overall x-ray detector efficiency, including the solid angle factor and the aluminum absorption factor, is

$${}_{88\text{ keV}}\langle\epsilon\Omega\delta/4\pi\rangle_x = 0.127 \pm 0.013.$$

A computation of the expected efficiency of the detector for a point source located at the center of the target yields

$$(\epsilon\Omega\delta/4\pi)_x = 0.166,$$

while the measured value for this point is

$$(\epsilon\Omega\delta/4\pi)_x = 0.157 \pm 0.016,$$

in good agreement with the calculated value. The discrepancy is less than the 10% error in the source calibration.

It is noted here that, in the region of x-ray energies of interest in this experiment ( $\langle\epsilon\Omega\delta/4\pi\rangle_x$  is very nearly a constant. As  $Z$  is varied and the  $K$  x-ray energy consequently varies, any added attenuation in the thin Al vacuum wall is very nearly compensated for by a slightly improved detection efficiency in the x-ray detector.

The width of the 88-keV Cd<sup>109</sup> photopeak was studied as were the  $K$  x-ray peaks from the actual targets used. The latter were found both by irradiating all targets of

interest with 0.51-MeV annihilation quanta, and by exposing the targets to the actual experimental beta flux, and subtracting from the observed x-ray spectra the result of the same experiment done with an Al target. In each case, the result was a peak at the expected x-ray energy with about 50% full width at half-maximum. These observed x-ray peaks agreed with other calibration points for the x detector, and were at the expected<sup>23</sup> position. The x-ray scale was calibrated by the 0.51-MeV annihilation peak, the 127-keV gamma of Co<sup>57</sup> and the 88-keV gamma of Cd<sup>109</sup>. The selection of biases in the x-ray channel was further facilitated by the direct observation of the characteristic  $K$  x-ray peak of each target.

The detection efficiency of the gamma detector was measured using a calibrated source of Na<sup>22</sup>. This source was used to calibrate the detector for both the 1.28- and 0.51-MeV gamma rays. The former is nearly equal to the energy of a hard gamma from SQA and so represents an experimental determination of a quantity closely related to  $\langle\epsilon\Omega\delta/4\pi\rangle_\gamma$ . The 0.51-MeV efficiency is used to compute the positron flux from the observed target-connected 0.51-MeV rate.

The results are:

$$\langle\epsilon\Omega\delta/4\pi\rangle_{0.51} = (1.91 \pm 0.2) \times 10^{-2},$$

$$\langle\epsilon\Omega\delta/4\pi\rangle_{1.28} = (6.81 \pm 0.7) \times 10^{-3}.$$

The errors in these two quantities are mainly due to source calibration, and hence are correlated.

Here again, a calculation of the efficiency is in good agreement with the measured values. For example ( $\epsilon\Omega\delta/4\pi$ )<sub>0.51</sub>, for a source at the center of the target, was calculated to be  $1.96 \times 10^{-2}$ , while the measured value was  $(1.72 \pm 0.17) \times 10^{-2}$ .

The efficiency of  $\gamma$  detection in the photopeak was determined as a function of gamma-ray energy by logarithmic interpolation between the 0.51-MeV and 1.28-MeV calibrated points. This interpolation seems quite reasonable in view of the results of Miller *et al.*<sup>24</sup> At the lower bias level of 1.05 MeV, the photoefficiency vs  $E_\gamma$ , including the effect of the finite resolution (9%) of the photopeak, was found by integrating an assumed Gaussian shape for the photopeak. The results are shown in Fig. 3.

The Compton efficiency, never more than 20% of the total efficiency, was estimated by assuming that the relative pulse-height spectrum at any gamma-ray energy of interest (e.g.,  $1.05 \leq E_\gamma \leq 1.36$  MeV in lead) is the same as that at 1.28 MeV. The Compton portion of this spectrum was then integrated down to a fraction of the maximum energy appropriate to the 1.05-MeV bias level for the gamma-ray energy considered. This pro-

<sup>23</sup> A. H. Compton and S. K. Allison, *X rays in Theory and Experiment* (D. Van Nostrand Company, Inc., Princeton, New Jersey, 1948), 2nd ed.

<sup>24</sup> W. Miller, J. Reynolds, and W. Snow, *Rev. Sci. Instr.* **28**, 717 (1957).

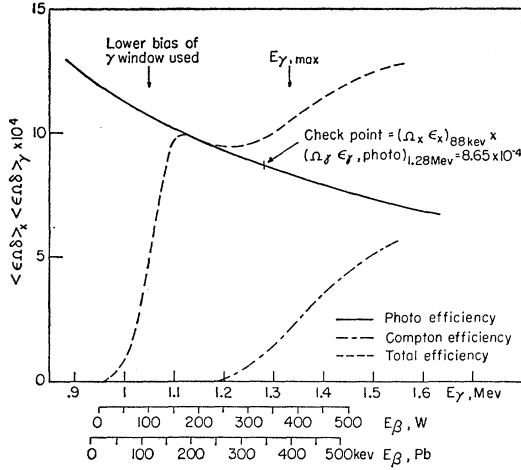


Fig. 3. Detection efficiency vs gamma-ray (or beta-ray) energy.

cedure is in error, but in view of the small contribution of the Compton effect to the total gamma detection efficiency ( $< 20\%$  even for the highest  $\gamma$  energies) it was felt that a more elaborate calculation was unwarranted.

The total  $\gamma$  efficiency was taken to be the photo-efficiency plus the Compton efficiency. The results of this semiempirical determination of the gamma-detector efficiency vs  $E_\gamma$  are shown in Fig. 3.

The gamma-ray energy scale was calibrated by the 0.51-Mev annihilation peak, the 1.28-Mev  $\text{Na}^{22}$  nuclear gamma, and the 0.908- and 1.85-Mev gammas from  $\text{Y}^{88}$ .

## V. COMPARISON WITH THEORY

Assume that a monoenergetic beam of  $N$  positrons per second at energy  $E_0^+$  is incident upon a target of atomic number  $Z$ . As these positrons penetrate into the target their energy decreases, and the number of positrons also decreases due to annihilation in flight and due to backscattering (which is a function of  $Z$ ). Hence, at energy  $E^+$ , there are a number of positrons,  $N$ , which is a function of  $E_0^+$ ,  $E^+$ , and  $Z$ ; i.e.,  $N = N(E_0^+, E^+, Z)$ .

Since, for a given target, the energy of the positrons  $E^+$ , and the energy of the resulting hard gamma from SQA,  $E_\gamma$ , are related via Eq. (1), all energy-dependent terms may be written as functions of either energy. A comparison of the  $E_\gamma$  and  $E^+$  scales for Pb and W is shown in Fig. 3.

Let the cross section per atom for SQA be  $\sigma(E, Z)$ . The number of annihilations occurring while the positrons lose energy  $dE$  is

$$dN = \left[ N(E_0, E, Z) n \sigma(E, Z) dE / \frac{dE}{dS}(E, Z) \right], \quad (2)$$

where  $dE/ds$  is the energy loss per unit path length of positron travel, and  $n$  is the number of atoms per unit volume, given by

$$n = A\rho/M, \quad (3)$$

where  $A$  is Avagadro's number,  $\rho$  is the mass per unit volume of the target, and  $M$  is the mass of a gram atom of target.

In order to identify SQA we observe the  $K$  x ray and the annihilation  $\gamma$  from each event. The x-ray and gamma-ray detectors have intrinsic efficiencies  $\langle \epsilon \Omega \delta / 4\pi \rangle_x$  and  $\langle \epsilon \Omega \delta / 4\pi \rangle_\gamma$ , respectively.

There is a target attenuation of the  $\gamma$  and  $K$  x-ray existing from the target. The attenuation for the  $\gamma$  ray is negligible and will be ignored. The attenuation of the x ray depends upon  $Z$  and the depth at which the annihilation takes place. The attenuation of the  $K$  x ray is important, and will be included as a term,  $\xi(Z, E_0, E)$ , equal to the fraction of  $K$  x rays exiting from the target. The fraction of single-quantum events detected is thus

$$\langle \epsilon \Omega \delta / 4\pi \rangle_x \langle \epsilon \Omega \delta / 4\pi \rangle_\gamma \xi(E_0, E, Z). \quad (4)$$

For the observed SQA rate, Eqs. (2)-(4) yield

$$R = \frac{A\rho}{M} \int_{E_{\min}}^{E_{\max}} \left[ \langle \epsilon \Omega \delta / 4\pi \rangle_x \langle \epsilon \Omega \delta / 4\pi \rangle_\gamma \xi(E_0, E, Z) \times N(E_0, E, Z) \sigma(E, Z) / \frac{dE}{dS}(E, Z) \right] dE. \quad (5)$$

In evaluating the integral shown in Eq. (5), a large number of approximations were made. These are discussed below.

We neglect the extremely small effect of the variation in the geometry of the source of SQA events, due to variations as a function of  $E^+$  of the average depth of penetration of the positrons. We are effectively neglecting the depth of penetration of the positron compared to the target-detector separation. The  $K$  x-ray energy for a given target is not a function of  $E^+$ , hence,  $\langle \epsilon \Omega \delta / 4\pi \rangle_x$  may be removed from the integral. Also, as mentioned previously,  $\langle \epsilon \Omega \delta / 4\pi \rangle_x$  is very nearly constant over the region of  $Z$  of interest, hence, it is considered to be a constant when comparing the predicted rates in two elements.

The x ray, in exiting from the target, is attenuated. The fraction of  $K$  x rays which exit from the target,  $\xi(Z, E_0^+, E)$  depends on the depth of positron penetration into the target (and hence on  $E_0^+$  and  $E$ ) as well as on the x-ray attenuation length (and hence  $Z$ ). The term  $\xi(Z, E_0^+, E)$  depends on the details of the penetration of the  $\beta^+$  beam into the target. Instead of a proper treatment of this term (which typically, gives rise to a 20% decrease in the observed rate of SQA) we have separately estimated the energy average,  $\langle \xi(Z, E_0) \rangle$  for the geometry of this experiment. This removes the term from the integral in Eq. (5) and leaves it as a function of  $Z$ . The errors in this calculation were estimated and included in the final errors.

Values of  $dE/dS(E, Z)$  taken from the NBS data<sup>25</sup>

<sup>25</sup> Ann T. Nelms, National Bureau of Standards Circular No. 577 (U. S. Government Printing Office, Washington, D. C., 1956).

were used.  $N(E, Z)$  was computed assuming a monoenergetic incident beam of positrons. (The error due to this assumption was shown to be negligible.) Corrections for backscattering were made using the data of Seliger *et al.*<sup>26</sup>  $N(E)$  was also corrected approximately for 2-quantum annihilation in flight. The use of Seliger's data for backscattering represents a possible major source of error in this computation. These data hold for 90° incidence, while in the present experiment angles of incidence half this large are typical. The backscattering contributes  $-0.7$  powers of  $Z$  to the dependence of  $R$  on  $Z$ . This may be in error by a large fraction. An error of 30% in the backscattering was allowed.

It was assumed that the positron direction becomes isotropic after a negligible penetration length. This should occur for penetration distances corresponding to a 5% energy loss.<sup>15</sup> Hence, the cross sections considered were averaged over all angles of observation, and the expected angular distribution<sup>16</sup> was *not* used.<sup>27</sup>

The rate given by Eq. (5) was computed for Pb and W. Two theoretical cases were considered for  $\sigma(E, Z)$ . One was the Born approximation,<sup>7</sup> which is proportional to  $Z^5$ . The Born approximation, therefore, is used in the form

$$\sigma(Z, E) = \sigma_0(E) \times Z^5.$$

The second cross section considered was that calculated by Jaeger and Hulme<sup>10</sup> using explicit Coulomb wave functions. This calculation was unfortunately done only for lead. A  $Z^5$  dependence was also assumed here. (What is needed is a cross section computation like that of Jaeger and Hulme comparing, for example, Pb and W.)

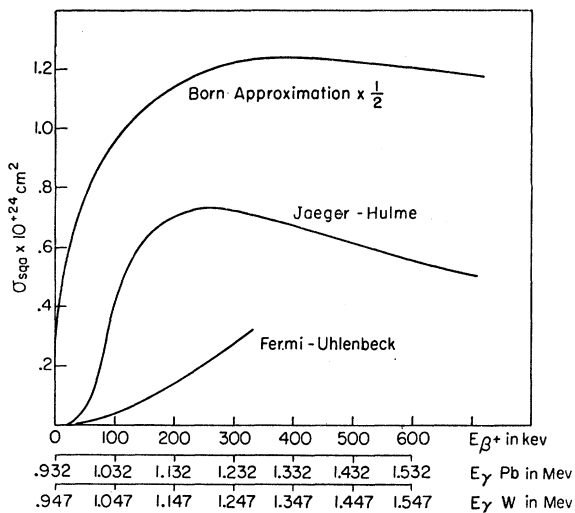


FIG. 4. Cross section, per Pb atom, for SQA.

<sup>26</sup> H. Seliger, Phys. Rev. **78**, 491 (1950).

<sup>27</sup> Due to nonconservation of parity in beta decay a preferred direction does persist, namely the direction of polarization of the positron beam. This preferred direction persists even after positron momenta have become isotropic. However, no dependence of  $\sigma$  on the angle between the gamma rays and the preferred spin direction is expected.

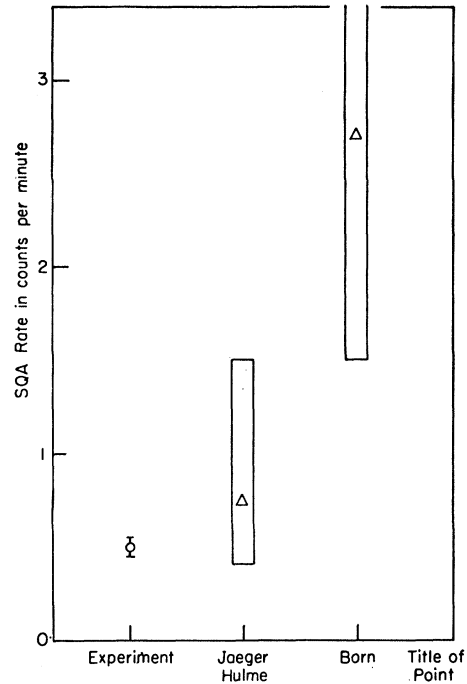


FIG. 5. Absolute magnitude of SQA rate. The theoretical points were computed using the Jaeger-Hulme<sup>10</sup> and Born<sup>9</sup> approximation cross sections shown in Fig. 4. The theoretical points include an estimate of the maximum systematic error (oblong box). The flags shown on the experimental point include only the statistical counting error.

Figure 4 is a plot of the energy dependence of  $\sigma_{JH}$  and  $\sigma_B$ . Also shown is the energy dependence of the cross section for SQA computed by Fermi and Uhlenbeck<sup>11</sup> using nonrelativistic wave functions.

The results for the predicted counting rates in lead were

$$R_{Pb,B} = 2.71 \text{ counts/min,}$$

for the Born approximation and

$$R_{Pb,JH} = 0.75 \text{ counts/min,}$$

for the Jaeger-Hulme cross section. These are compared to the experimental results in Fig. 5. The systematic error shown in Fig. 5, ( $-45\%$ ,  $+100\%$ ), is the estimated upper limit of the errors introduced by the approximations made in evaluating Eq. (5). These errors are shown as flags on the "theoretical values."

The  $Z$  dependence following from the assumptions listed above was reached by interpolating between and extrapolating from the calculated Pb and W points. This  $Z$  dependence is shown in Fig. 6. Again, the systematic errors attributed to the theory are due to errors in evaluating Eq. (5). In this case, however, since only the  $Z$  dependence is of interest, the data are normalized to lead, and only those systematic errors effecting  $Z$  dependence are shown.

Approximately, the  $Z$  dependence terms have the following order of importance. In Eq. (5), the dominant

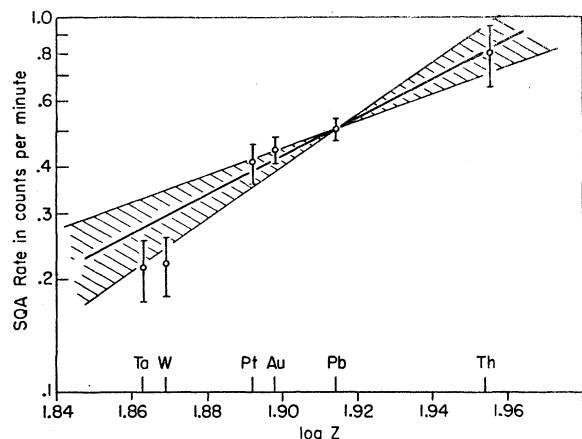


FIG. 6.  $Z$  dependence of counting rate. The heavy central line is the theoretical result assuming a  $Z^5$  dependence of cross section. The shaded area about the theoretical line represents the estimate of the maximum effect of systematic errors on  $Z$  dependence. The flags on experimental points represent statistical counting errors only.

$Z$  dependence is of course the  $Z^5$  dependence of  $\sigma$ . The next strongly  $Z$  dependent factor is  $dE/dS$ . If we include this but neglect all other  $Z$  dependences, a rate proportional to  $Z^4$  is expected. Other  $Z$ -dependent factors of note are the backscattering dependence of  $N(E, Z)$  and the attenuation of  $K$  x rays leaving the target,  $\xi(\epsilon_0, E, Z)$ . Together, these two terms contribute approximately  $-0.7 + 0.6 = -0.1$  powers of  $Z$  to the  $Z$  dependence.

The results of the computation of  $R$  vs  $E_0^+$  is shown in Fig. 7. Here again, since only a relative measure of  $R$  is important, the errors shown include only those

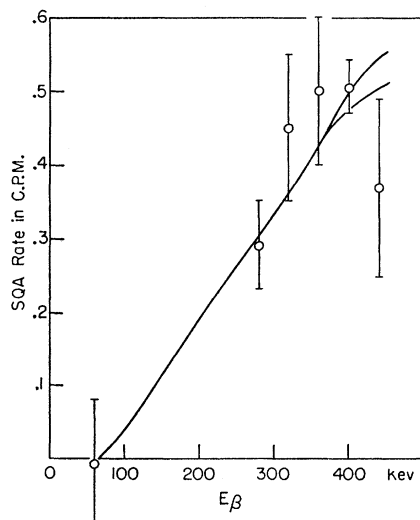


FIG. 7. Dependence of SQA counting rate on  $E_0^+$ . The curve is the theoretical result assuming the energy dependence of the Jaeger-Hulme cross section.<sup>10</sup> The theoretical split on the upper right of the curve shows the uncertainty in theoretical value due to only those terms which affect energy dependence. The flags on the experimental points represent statistical counting errors only.

systematic errors effecting dependence of  $R$  on  $E_0^+$  for a single target. The data are normalized to the 400-kev point in Pb.

## VI. DATA TAKING

After the calibration described in Sec. IV, several exploratory runs were made to investigate the signal and noise rates. On the basis of these early runs<sup>15</sup> the biases were decided upon. The x-ray biases were chosen to include 80% of the  $K$  x-ray peak. The gamma biases were chosen to include 1.05 to 1.40 Mev. Later investigations indicated that the upper gamma bias may have been mistakenly set at 1.35 Mev. This uncertainty is included in the curve of Fig. 7 representing the computed rates vs  $E_0^+$ .

The first SQA signal investigated was that for Pb. The lead target was inserted in position and data were taken for 30 min. During this period data were simultaneously taken on the  $K$  x-ray peak, and at about twice the  $K$  x-ray peak. The latter data were useful in investigating the background dependence on  $Z$  and on x-ray window position. The lead target was then replaced by the Al target, while all bias levels and the magnetic field remained the same. Aluminum data was then taken for 30 min. The rate for Pb, minus the Al rate, was taken to be the signal rate (see Sec. VII). The above sequence of data taking was repeated until the desired statistics had been obtained.

In the  $Z$  dependence series of data a similar procedure was followed. Whenever data were taken on a target, "off  $K$  x-ray" data were simultaneously taken, and then an Al run was made with the same biases. When a change of  $Z$  was made, the  $K$  x-ray window was not changed. Instead, the high voltage on the x-ray counter was varied so that the  $K$  x-ray peak of the element being investigated was centered in the x-ray window. In this way approximately the same fraction of each  $K$  x-ray peak was observed. This fraction had to be corrected for the change in x-ray detector resolution as a function of  $K$  x-ray energy. Each  $Z$  data-taking run was followed by an Al run at the same biases. In each  $Z$ -dependence run, three elements were used in addition to Al. In order to cover the entire spectrum of  $Z$ , the vacuum system was opened, and new targets inserted. In each case, Pb and Al were included in the selection of targets. In the  $Z$ -dependence data, as in the data on absolute rate in lead, the counting rate with target  $Z$  minus the counting rate in Al was taken as the SQA signal. The thorium data received special handling due to the additional signal from the natural radioactivity of the target. The field was periodically reversed and the thorium rate measured in the absence of positron flux.

In the data on the dependence of the counting rate on beta energy, Pb and Al rates were again measured, with x-ray windows on and above the  $K$  x-ray peak of Pb. The magnetic field was varied, and Pb-Al differences were taken at each desired field point. The data were normalized to the positron flux.



The  $K$  x-ray dependence was studied for a lead target and  $E_0^+ = 400$  kev. All of the above-mentioned runs provided data on the SQA rate with the x-ray window on the  $K$  x-ray peak vs the SQA rate with the window above the peak. A separate run was made to compare the SQA rate on the  $K$  x-ray peak to that below the peak. Narrower x-ray windows had to be used, and the data of this run then necessarily had to be normalized to equal fractions of the  $K$  x-ray peak with the previous data. The comparison of the data on the  $K$  x-ray peak with that below the peak used an x-ray window which accepted 0.6 of the  $K$  x rays rather than 0.8. The data were corrected accordingly. Other than this correction, all operations were similar to previous runs.

During the data taking, it was found that the singles rates were excellent stability monitors (in the x-ray channel on the  $K$  x-ray peak, and in the gamma-ray channel the rate from 1.05 Mev to about 1.40 Mev). Changes of 2% in gains or in magnetic field were easily detectable. In addition, the 0.51-Mev peak was periodically checked.

## VII. BACKGROUNDS

The major background was a  $Z$ -independent, non  $K$  x-ray connected event. Data, taken at x-ray energies above the  $K$  x-ray peak (hereafter called the "off  $K$  x-ray rate") in all targets, indicate a background varying more slowly than the 0.01 power of  $Z$ . The ratio of this background on any target to that on the Al target was typically  $1.0 \pm 0.1$ . This  $Z$ -independent background was about  $\frac{1}{3}$  of the total rate in lead. It was eliminated from the SQA rate by subtracting, in each case, the rate in aluminum from the rate in the target of interest.

One major source of this background is a hard gamma from 2-quantum annihilation in flight in chance pile-up, in the gamma counter, with a 0.51-Mev gamma from a two-quantum annihilation at rest. The other 0.51-Mev gamma from the annihilation at rest or the soft gamma from two-quantum annihilation in flight is detected via a Compton collision in the x-ray detector, such that the resulting pulse falls in the x-ray window. An investigation of the background in Al, as a function of x-ray window position, indeed showed the variation expected from Compton-detected 0.51-Mev gammas. Furthermore, the resolving time of the gamma-ray detector for pile-up events, was decreased at an early point in the experiment, and the SQA rate remained unchanged while the "off  $K$  x-ray rate" decreased, indicating that the observed off  $K$  x-ray rate was due to a pile-up event in the gamma counter. The event described above probably accounts for about  $\frac{2}{3}$  of the "off  $K$  x-ray rate."

A second major component of this background rate is present even in the absence of positron flux. (i.e., when the spectrometer field is reversed). It is due to cosmic rays and to the 1.28-Mev  $\text{Na}^{22}$  nuclear gamma ray, and accounts for the remaining  $\frac{1}{3}$  of the "off  $K$  x-ray rate." The event described above, the field-

reversed rate, and any other  $Z$ -independent rate, are subtracted by taking  $R(Z) - R(\text{Al})$  for each point.

We now consider other possible sources of coincidence counts. The simple chance coincidence rate due to uncorrelated x and gamma pulses was computed and then measured using 2 separate gamma sources. In both cases, it was found to be more than a factor of 10 below the lowest rates involved in the experiment.

A  $Z$ -dependent event which is not  $K$  x-ray connected, and therefore would be observed in the "off  $K$  x-ray" run, is some pile-up event in the gamma channel in coincidence with a bremsstrahlung quantum in the x detector. In Pb, where this effect might be expected to be large, it might give a background in the "on  $K$  x-ray" runs and half this background in the "off  $K$  x-ray" run. This type of background is shown to be negligible by the upper limit of the  $Z$  dependence of the "off  $K$  x-ray" background. This limit indicates that a background varying as  $Z^2$  is less than 10% the "off  $K$  x-ray" rate. This must be compared to an "on  $K$  x-ray" rate 3 times the off rate. Thus 20% of the "off  $K$  x-ray rate" is an upper limit for the contribution of this event to the "on  $K$  x-ray rate". We conclude that bremsstrahlung-connected processes are negligible, contributing less than 10% to the rates we call SQA.

One event which merits careful consideration is the following: A random coincidence in the gamma counter, between a hard  $\gamma$  from annihilation in flight, or from the  $\text{Na}^{22}$  source, and a 0.51-Mev  $\gamma$  satisfies the gamma bias requirements. The second 0.51-Mev  $\gamma$  or the soft gamma from annihilation in flight has a photoelectric interaction in the target, and the resulting x-ray is detected in the x detector. Such an event, if observed, is unusually insidious because it is  $K$  x-ray connected and has a high  $Z$  dependence. This rate was evaluated both from singles rates alone, and from the assumption that this background (without the photo interaction) accounts for all of our target connected "off  $K$  x-ray" counting rate (see below). In each case, the rate was more than an order of magnitude below the smallest SQA rates of interest.

In general, one method of estimating upper limits for any  $K$  x-ray connected rate was by assuming that all the "off  $K$  x-ray" rate was due to a related event without the  $K$  x-ray, and then scaling the results for the effects of the  $K$  x ray. For example, assume that the following is responsible for the off  $K$  x-ray rate of 0.3 counts/min. A hard gamma from annihilation in flight or from the  $\text{Na}^{22}$  plus a random 0.51-Mev  $\gamma$  pile up in the  $\gamma$  counter. The second 0.51-Mev  $\gamma$  is detected in the x-ray counter. Suppose this is the *entire* cause of the off  $K$  x-ray rate. Then the  $K$  x-ray connected related rate is due to the 0.51-Mev quantum having a photoelectric interaction in the target. The ratio of this rate to the off  $K$  x-ray rate is

$$R_{K \text{ x-ray connected}}/R_{\text{off } K \text{ x ray}} = f_1 \times E_x/E_{0.51},$$

where  $f_1$  is the fraction of 0.51-Mev gammas having a photoelectric interaction while exiting from the target,  $E_x$  is the efficiency for detecting the resulting  $K$  x ray and  $E_{0.51}$  is the efficiency for detection of the original 0.51-Mev  $\gamma$  (i.e., a gamma back to back with the one which entered the  $\gamma$  counter). This computation indicates that the  $K$  x-ray connected rate from this process is no more than 15% of the off  $K$  x-ray rate, and hence no more than 7.5% of the rate attributed to SQA. (Recall that the SQA rate is twice the off  $K$  x-ray rate.) The suspected  $K$  x-ray connected backgrounds were handled in this fashion. In each case, the resulting  $K$  x-ray connected rate to be expected was an order of magnitude or more below the observed  $K$  x-ray connected rate.

Rates involving a  $K$  x ray which arises from a  $K$  ionization of a target atom by the incident beta were evaluated semiempirically. An upper limit on the efficiency of producing such  $K$  x rays was computed from measured  $K$  x-ray peaks, resulting from the known incident beta flux. The extreme limit, considering all  $K$  x rays to arise from beta collisions rather than photoelectric effect of 0.51-Mev gammas, was used. In each case, the rates were more than an order of magnitude below SQA rates of interest.

Two-quantum annihilation in flight is strongly rejected by the  $\gamma$ -energy requirements. In fact, for the  $E_0^+ = 280$ -keV point (Fig. 7), it is completely rejected. It is furthermore discriminated against for all data points by the poor detection efficiency of the less energetic quantum in the x-ray detector. As a result of this it should be a very small fraction of the spurious rate in this experiment even for those points for which it can be detected. It should furthermore be nearly  $Z$  independent and so should be removed by the Al subtraction (see Sec. VIII). If any large fraction of the "off  $K$  x-ray" rate were due to simple 2-quantum annihilation in flight, one would expect the rate to rise rapidly as  $E_0^+$  is increased, since more of the hard quanta would be seen above our lower gamma bias. No such "off  $K$  x-ray" rise in rate is observed. Instead the "off  $K$  x-ray" rate appears to vary as the square of the beta flux as would be expected from the events which we described at the beginning of this section. We conclude that there is no evidence that a measureable fraction of the background is due to simple two-quantum annihilation in flight. *A fortiori* there is no effect of simple two-quantum annihilation in flight on our SQA rate.

Two-quantum annihilation in flight with a  $K$  electron is neither removed by the Al subtraction, nor is it discriminated against by the x detector. As described earlier in this section, this rate is semiempirically eliminated by assuming that the *entire* "off  $K$  x-ray" rate is due to two-quantum annihilation in flight, and scaling this rate down for the annihilation of only  $K$  electrons and the subsequent detection of the  $K$  x ray. As in the case of other  $K$  x-ray connected backgrounds,

this calculation indicates the expected rate is an order of magnitude below the observed  $K$  x-ray connected rate. Furthermore, the energetics of two-quantum annihilation with a  $K$ -shell electron indicate that the resulting hard  $\gamma$  ray should be unobservable due to our lower gamma ray bias. On this basis alone we may conclude the  $K$ -connected two-quantum contribution is negligible

## VIII. RESULTS

We have described in Sec. V the approximations used in arriving at a graphical integration of Eq. (5). Figure 5 shows the results for the computation. The theoretical results are displayed with indications of the estimated maximum errors introduced by the uncertainties and approximations described in Sec. V. Figure 5 also shows the result for the counting rate in lead at  $E_0^+ = 400$  keV,  $N_0 = 6.6 \times 10^4$ /sec. The experimental point includes statistical errors shown by the usual "flags." It is seen that if all of our calculational estimates are as bad as we believe they can be, we may still conclude that the counting rate is much below the Born approximation predicted rate. It is, however, within the range of possible agreement with the Jaeger-Hulme<sup>8</sup> cross section. The disagreement with the Born approximation is not surprising. Heitler<sup>7</sup> points out that this computation should be valid when  $2\pi Ze^2/\hbar v_{\pm} \ll 1$ . In the present case these quantities are both approximately equal to 3. The dominant errors in this experiment are the systematic errors introduced by our particular geometry. The lack of 90° incidence of the positron beam, in particular, introduces a large uncertainty in the back-scattering coefficient. Further experimental work, in a more easily analyzed geometry will decrease the important systematic uncertainties, probably by a factor of 3. In addition, a comparison of rates for geometries in which the gamma comes off in the direction of the incident positron, and in a direction perpendicular thereto, should experimentally eliminate the question of how isotropic are the momenta of the positrons.

Figure 6 shows the expected  $Z$  dependence based upon the assumption of a  $Z^5$  dependence of the atomic cross section. The theoretical behavior is shown along with (shaded area) the maximum estimated errors due to approximations made in computing the SQA rates. Only those errors bearing upon the  $Z$  dependence are shown, and the absolute rate is normalized to lead. The data fit the  $Z^5$  dependence. The semiempirical correction factor of Heitler<sup>9</sup> indicates however, that a cross section proportional to about  $Z^{3.8}$  is to be expected. The data are a poor fit to the  $Z^{3.8}$  theory. (For example, the maximum slope allowed by the  $Z^{3.8}$  dependence plus the estimated maximum systematic error is very little different from the central theoretical line for  $Z^5$ , in Fig. 6.) It would be surprising, theoretically, if the  $Z$  dependence were not markedly less than the Born approximation's  $Z^5$  at the energies used in this experiment. In the second round of this experiment an attempt

will be made to reduce the systematic errors in the  $Z$  dependence, so that a stronger experimental statement can be made.

Figure 7 shows the expected and measured dependence on  $E_0^+$  of the counting rate in lead. The data in this run are insufficiently accurate to distinguish between the Born approximation and Jaeger-Hulme energy dependence. Only the latter is shown. Data were taken at incident positron energies of 60, 280, 320, 360, 400, and 440 keV. The low point at 440 keV may be due to a statistical fluctuation, or due to a small error in the upper level of the window in the  $\gamma$  differential discriminator, as mentioned at the beginning of Sec. VI. It is comforting to note that the SQA rate at the 60-keV point is zero despite the fact that *the actual  $\beta^+$  flux at the 60-keV point is the same as that at 400 keV*. The observed counting rate for true SQA must be zero at the lower incident kinetic energy due to the lower  $\gamma$  discriminator level. At the lower  $E_0^+$ , all rates except SQA, and two-quantum annihilation in flight are very nearly the same as at the higher  $E_0^+$  settings. The 280-keV point is also worthy of note, since at this point 2-quantum annihilation in flight (with or without  $K$ -shell annihilation) cannot be detected directly in the  $\gamma$  channel. The fact that an SQA rate, consistent with that at other points, is observed argues against any serious contamination of our data by two-quantum annihilation in flight.

Figure 8 shows the expected and measured dependence of the SQA rate on the setting of the x-ray window. The expected rate assumes the counting rate is due entirely to SQA with  $\sigma = 0.65 \sigma_{JH}$ . Figure 8 alone demonstrates clearly that we are indeed observing a  $K$  x-ray connected event.

To summarize: It is clear from the data that we are observing a  $K$  x-ray connected event. The off  $K$  x-ray data is, within experimental error, independent of  $Z$ . All  $K$  x-ray events which might reasonably be expected to compete with SQA have been shown to be negligible (a) by direct computation and (b) by assuming that the rates observed with the x-ray window set above the  $K$  x-ray peak are entirely due to a closely related (non  $K$  x-ray connected) event, and then scaling this event for the few terms relating it to the  $K$  x-ray connected rate. Within experimental error the resulting signal attributed to SQA in the above work has the expected dependence on  $E_0^+$ . In particular, it is zero for  $E_0^+ = 60$  keV although the positron flux there is the same as at

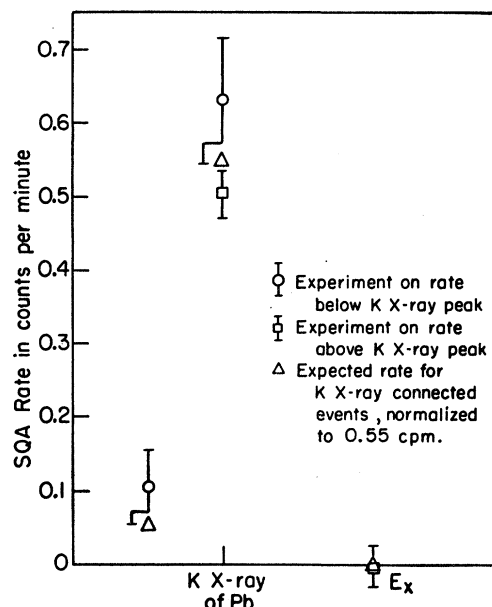


FIG. 8. Dependence of SQA rate on x-ray energy.

the 400-keV point. Also, the SQA rate is measurable for  $E_0^+ = 280$  keV although the 2-quantum annihilation in flight is undetectable there. Finally, a steep  $Z$  dependence is observed. This is characteristic of SQA and not, e.g., two-quantum annihilation in flight, or indeed any other event except the photoelectric effect.

We conclude that we have observed single-quantum annihilation of positrons and that it occurs in lead with a cross section equal, within a factor of 2, to the Jaeger-Hulme<sup>10</sup> cross section. The  $Z$  dependence appears somewhat too high.

With the help of the data collected here, the experiment will be redesigned to provide a more favorable geometry so that the systematic errors may be greatly reduced. A thin-target experiment will also be attempted in order to measure the angular distribution of the gamma rays with respect to the beta direction. It does not appear feasible, at present, to measure the gamma-ray polarization.

We wish to express our thanks to M. Meer for his help in the early design stages of this experiment.<sup>28</sup>

<sup>28</sup> M. Meer, S.B. thesis, Brandeis University, Waltham, Massachusetts, 1956 (unpublished).